Tensor Product Type Polytopic LPV Modeling of Aeroelastic Aircraft

Béla Takarics, Alexandra Szöllősi and Bálint Vanek
Systems and Control Lab
Institute for Computer Science and Control
Hungarian Academy of Sciences
Kende u. 13-17.
1111 Budapest, Hungary
+36 1 279 6000 / 6288
{takarics.bela, szollosi.alexandra, vanek.balint}@sztaki.mta.hu

Abstract—**In order to improve fuel efficiency, future aircraft will have reduced weight and increased wingspan. Such aircraft require active control systems to suppress ASE effects. ASE systems are often modeled in the grid based linear parameter-varying (LPV) framework, which captures the parameter varying dynamics. The controller is generally synthesized by solving Linear Matrix Inequalities (LMIs) for the LPV model. Selecting the grid density for such control synthesis approach requires special attention. On the one hand, a too coarse grid might not capture the parameter variation of the dynamics accurately enough. On the other hand, solving LMIs for too dense grid can lead to numerical issues and computational cost. This is usually relaxed by synthesizing the controller for a coarser grid and the stability and performance are verified for a denser grid. A possible remedy for this drawback of grid-based LPV models is polytopic LPV representation. In such case the LMIs need to be solved only for the vertex systems of the convex polytopic hull. Various types of convex polytopic models can be obtained by Tensor Product (TP) model transformation. The aim of the paper is to derive polytopic models for ASE vehicles and to apply these models for flutter suppression control design. The goal is to have a small number of vertex systems and sufficient accuracy while keeping the conservativeness of polytopic modeling low. The aircraft under consideration is the mini MUTT (Multi Utility Technology Testbed) vehicle. Based on the polytopic representation a stabilizing state feedback controller and observer is synthesized. The effectiveness of the resulting control design is verified through numerical simulations.**

TABLE OF CONTENTS

1. INTRODUCTION

In order to improve fuel efficiency, future aircraft will have reduced weight and increased wingspan. These flexible aircraft show increased aeroservoelastic (ASE) effects. Aeroelastic flutter involves the adverse interaction of aerodynamics with structural dynamics and produces an unstable oscillation requiring active control systems to suppress ASE effects [1]. ASE systems are often modeled in the linear parameter-varying (LPV) framework [2], which captures the parameter varying dynamics of the aircraft. The LPV model of the nonlinear plant is generally obtained by Jacobian linearization about a family of equilibrium (*trim*) points. This leads to a "grid-based" LPV system [3]. The controller for grid based LPV systems is then synthesized by solving Linear Matrix Inequalities (LMIs) [4, 5]. Selecting the grid density for such control synthesis approach requires special attention. On the one hand, a too coarse grid might not capture the parameter variation of the dynamics accurately enough. On the other hand, solving LMIs for too dense grid can lead to numerical issues and computational cost. This is usually relaxed by synthesizing the controller for a coarser grid and the stability and performance are verified for a denser grid. There are two LPV approaches that lead to more computationally tractable LMI conditions. These are the linear fractional transformation (LFT) based LPV systems [6, 7] and the polytopic type LPV systems [8]. This paper focuses on the polytopic based approach.

A recently proposed numerical method capable of transforming LPV systems into convex polytopic forms is the Tensor Product (TP) model transformation [9, 10]. It generates the higher-order singular value decomposition (HOSVD) [11] based canonical form of LPV models. In addition, it is capable of generating various types of convex representations for the same model [12]. Based on the higher-order singular values the TP model transformation offers a trade-off between the complexity of the LMI-based control design and the accuracy of the resulting TP model [12]. ASE related applications of the TP model transformation can be found in [13–16].

The aim of the paper is twofold. First, the goal is to derive polytopic models of ASE aircraft via TP model transformation. It is crucial to obtain a polytopic model with small number of vertex systems and sufficient accuracy while keeping the conservativeness of polytopic modeling low. Second, a polytopic observer based state feedback controller is designed that stabilizes the ASE aircraft. This way the flutter boundary can be expanded with active flutter suppression. The specific aircraft under consideration is the mini MUTT (Multi Utility Technology Testbed) vehicle [17]. The mini MUTT is designed such that it exhibits strong coupling of rigid body dynamics and structural dynamics at low airspeeds.

The paper is organized as follows. The mini MUTT aircraft is described in Section 2, followed by the Tensor Product model transformation based theoretical concepts in Section 3. The polytopic control design steps are given in Section 4, which

978-1-5386-2014-4/18/$31.00

is followed by TP type polytopic model of the mini MUTT model in Section 5. The numerical results of the control design are given and evaluated in Section 6. Last, the results are summarized in Section 7.

2. The mini MUTT Aircraft

The aircraft under consideration is the mini MUTT (Multi Utility Technology Testbed) vehicle, built at the University of Minnesota. It is a remote-piloted flying wing aircraft with a wing span of $3m$ and a total mass of about $6.7kg$. The design closely resembles Lockheed Martin's Body Freedom Flutter vehicle [18] and NASA's X56 MUTT aircraft [19]. The mini MUTT is designed such that it exhibits strong coupling of rigid body dynamics and structural dynamics at low airspeeds. Flutter occurs above the airspeed of $24m/s$. The mini MUTT aircraft with the control surfaces is depicted in Figure 1 [20]. The model has throttle and 8 control surfaces as inputs. Two control surfaces ($L3$, $R3$) are used as elevator, additional two surfaces ($L2$, $R2$) are used as aileron and the remaining four surfaces ($L1$, $R1$ - on body; $L4$, $R4$ - at wing tips) are used for flutter suppression. The aircraft has 18 sensors in total. 12 of these sensors are located at the center of gravity (CG) of the undeformed body. These measured outputs are the attitude angles ϕ and θ, angular rates p, q and r, accelerations a_x, a_y and a_z, absolute value of the ground speed without wind components V_s, angle of attack α, sideslip angle β and flight path angle γ. There are 6 additional accelerometers and angular rate sensors located at the middle of the wing and at the wing tips to measure the effects of elastic deformation. These are accelerometers $a_{z_{LfwMID}}$ and $a_{z_{RfwMID}}$, roll rate sensors p_{LOUT} and p_{ROUT} and pitch rate sensors q_{LOUT} and q_{ROUT}. Subscripts L and R designate the left or right side of the aircraft, MID and OUT stand for the middle and the tip of the wing and fw means forward of the elastic axis of the wing. It is important to point out that the coordinate systems of the sensors located on the wing are aligned with the sweep angle of the wing.

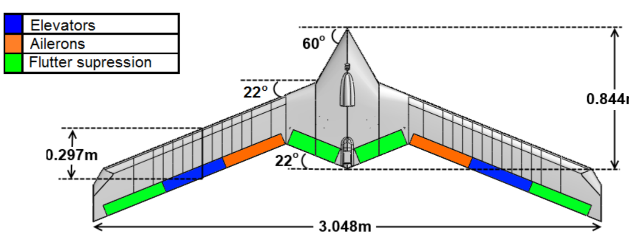

Figure 1: mini MUTT aircraft [21]

The ASE model of the mini MUTT aircraft considered in this paper is developed in [22]. The model is based on a subsystem approach [21]. The rigid body dynamics, aerodynamics and structural dynamics are modeled independently and later integrated into the ASE model. Two nonlinear models are developed in [22], a low order control oriented model and a higher order high fidelity model. The low order model consists of 33 states. The low order model is developed with the aim to capture the fundamental ASE behavior of the aircraft while keeping the number of states low enough for control synthesis. This is achieved by reducing the aerodynamics and structural dynamics subsystems before integrating them into the ASE model. The low order model is applied for the TP type polytopic modeling and control design. The full order is developed without reducing the subsystems and has 97 states. Therefore, this model is considered the high fidelity model. The 97 state nonlinear ASE model is used for validating the effectiveness of the resulting controller. Further specific details and results about the ASE model development of the mini MUTT aircraft can be found in [22].

3. TP Model of qLPV Systems

In this Section the concepts of quasi LPV (qLPV) models and TP model transformation will be described.

Linear Parameter Varying Models

Consider an LPV state-space model given as:

$$\begin{bmatrix} \dot{x}(t) \\ y(t) \end{bmatrix} = S(\rho(t)) \begin{bmatrix} x(t) \\ u(t) \end{bmatrix} \tag{1}$$

with $u(t) \in \mathbb{R}^{\mathbb{K}}$ input, $y(t) \in \mathbb{R}^{\mathbb{L}}$ output, $x(t) \in \mathbb{R}^{\mathbb{M}}$ state vector, $\rho(t) \in \Omega \subset \mathbb{R}^{\mathbb{N}}$ parameter vector with dimension N, where the parameter space $\Omega = \omega_1 \times \omega_2 \times \ldots \times \omega_N = [\omega_1^{min}, \omega_1^{max}] \times [\omega_2^{min}, \omega_2^{max}] \times \cdots \times [\omega_N^{min}, \omega_N^{max}] \subset \mathbb{R}^{\mathbb{N}}$ along each dimension $n = 1 \ldots N$ and parameter dependent system matrix $S(\rho(t)) \in \mathbb{R}^{\mathbb{O} \times \mathbb{I}}$, where $O = M + K$ and $I = M + L$. The system matrix $S(\rho(t))$ consists of:

$$S(\rho(t)) = \begin{bmatrix} A(\rho(t)) & B(\rho(t)) \\ C(\rho(t)) & D(\rho(t)) \end{bmatrix}$$

The dependence on time t is occasionally suppressed in the remainder of the paper to shorten the notation. The parameter vector ρ may include elements of the state vector x, in this case the system belongs to the class of quasi LPV (qLPV) models. Further parameter dependent channels, which can represent also various control performance requirements can be incorporated into $S(\rho)$.

TP Model Transformation and Polytopic TP Type Representation

sThe SVD for N-th-order tensors (termed as HOSVD) and the notation $\mathcal{X} \otimes_n \mathbf{U_n}$ was introduced by Lathauwer et al [11], with the core tensor $\mathcal{X}$ containing scalar values. In case of TP model transformation based applications, HOSVD is applied with notation $\mathcal{X} \underset{n \in N}{\boxtimes} \mathbf{U_n}$ to express the difference, that instead of scalar values, the elements of the core tensor $\mathcal{X}$ contain linear time-invariant (LTI) matrices [12, 23]. A more detailed discussion of the notations, operations and concepts are given in [11, 12, 23].

The system matrix $S(\rho)$ of (1) is reconstructed for any parameter ρ with the following polytopic structure:

$$S(\rho) = \sum_{r=1}^{R} w_r(\rho) S_r \tag{2}$$

The ordering $r = ordering(i_1, i_2, \ldots i_n, i_{n+1}, \ldots i_N)$, determines r as a linear index of the multilinear array index of the size $I_1 \times I_2 \ldots I_{n-1} \times I_{n+1} \ldots I_N$, $w_r(\rho) = \prod_{n=1}^{N} w_{n,i_n}(\rho_n(t))$ and $S_r = S_{i_1,\ldots,i_N}$. The canonical HOSVD based polytopic TP model form of (2) consists of [24–26]:

$$S(\rho) = \sum_{i_1=1}^{I_1} \cdots \sum_{i_N=1}^{I_N} \prod_{n=1}^{N} w_{n,i_n}(\rho_n) S_{i_1,\ldots,i_N} \tag{3}$$

which consists of weighting functions $w_n(\rho_n(t))$ and the parameter varying, singular value ordered orthonormal combination of Linear Time-Invariant (LTI) matrices $S \in \mathbb{R}^{\mathbb{O}\times\mathbb{I}}$ (termed as vertexes). With the compact tensor notation the canonical HOSVD based polytopic TP model form (3) results in:

$$S(\rho) = \mathcal{S} \underset{n\in N}{\boxtimes} w_n\left(\rho_n\right) \tag{4}$$

The core tensor's coefficients $\mathcal{S} \in \mathbb{R}^{\mathbb{I}_1\times\ldots\times\mathbb{I}_N\times\mathbb{O}\times\mathbb{I}}$ are constructed from the LTI vertex matrices $S_{i_1,\ldots,i_N}$, row vectors $w_n\left(\rho_n\right)$ from the univariate weighting functions $w_{n,i_n}(\rho_n)$, $i_n = 1\ldots I_N$ and ρ_n consists of the n-th element of vector ρ.

Definition 1 (Finite element polytopic TP model) The qLPV model (1) can be defined using a TP model structure as

$$\begin{bmatrix}\dot{x}\\ y\end{bmatrix} = \mathcal{S} \underset{n\in \mathrm{N}}{\boxtimes} w_n(\rho_n) \begin{bmatrix}x\\ u\end{bmatrix} \tag{5}$$

The $N+2$-dimensional core tensor $\mathcal{S} \in \mathbb{R}^{\mathbb{I}_1\times\cdots\times\mathbb{I}_N\times\mathbb{O}\times\mathbb{I}}$ is created from the LTI system matrices $S_{i_1,\ldots,i_N} \in \mathbb{R}^{\mathbb{O}\times\mathbb{I}}$. If a convex combination of the vertexes is defined by the weighting functions for all n, then

$$\begin{bmatrix}\dot{x}\\ y\end{bmatrix} = \mathcal{S} \underset{n\in \mathrm{N}}{\boxtimes} w_n^{Co}(\rho_n) \begin{bmatrix}x\\ u\end{bmatrix} \tag{6}$$

and the TP model consists of a polytopic representation. Thus the system matrix $S(\rho)$ is always contained in $co\{\forall n, i_n : S_{i_1,\ldots,i_N}\}$, where the LTI systems $S_{i_1,\ldots,i_N}$ are referred to as vertexes. The polytopic TP model is a higher structured polytopic representation since it can always be given as:

$$S(\rho) = \sum_{r=1}^{R} w_r^{Co}(\rho) S_r \tag{7}$$

Vertexes S_r are equivalent to the vertexes stored in tensor $\mathcal{S}$, as $S_r = S_{i_1,i_2,\ldots,i_n}$ and $w_r(\rho) = \Pi_{n=1}^{N} w_{n,i_n}(\rho_n)$. The finite index r is a linear equivalent of multidimensional indexes $i_1, i_2, \ldots, i_N$.

Definition 2 (Convex TP model) The polytopic TP model (5) is convex if its weighting functions $w_n(\rho_n)$, Co satisfy the following criteria:

$$\forall n, \rho_n : w_n(\rho_n) = 1 \tag{8}$$

$$\forall n, i, \rho_n : w_{n,i}(\rho_n) \in [0, 1] \tag{9}$$

The weighting functions are denoted as $w_n^{Co}(x_n)$, Co denotes convex. In this case, the polytopic TP model (5) is always within the convex hull defined by the elements, that is the LTI system matrices $S_{i_1,\ldots,i_N} \in \mathbb{R}^{\mathbb{O}\times\mathbb{I}}$ (vertexes) of the $N+2$-dimensional core tensor $\mathcal{S} \in \mathbb{R}^{\mathbb{I}_1\times\cdots\times\mathbb{I}_N\times\mathbb{O}\times\mathbb{I}}$.

Various special types of convex hulls can be defined through introducing further characteristics for the weighting functions, resulting in different shapes and tightness for the convex hulls [12, 23].

Definition 3 (SN type TP model) : The convex polytopic TP model is SN (Sum Normalized), if the sum of the weighting functions for all ρ_n is 1 for each dimension n.

Definition 4 (NN type TP model) The convex polytopic TP model is NN (Non-Negative), if the values of the weighting functions for all ρ_n are non-negative for each dimension n.

Definition 5 (NO/CNO type TP model) The convex polytopic TP model is a NO (Normal) type model, if its weighting functions are Normal, that is, if it satisfies (8) and (9), and the largest value of all weighting functions is 1 for each dimension n. Also, the convex TP model is CNO (Close to Normal), if it satisfies (8) and (9), and the largest value of all weighting functions is 1 or close to 1 for each dimension n.

Definition 6 (RNO type TP model) The convex polytopic TP model is Relaxed NO (RNO) type, if the largest values of all weighting functions are the same (note, that if the matrix is SN and NN type, then this value is always between 0 and 1) for each dimension n.

Definition 7 (INO type TP model) The convex polytopic TP model is an Inverse NO (INO) type, if the smallest value of all columns is 0 for each dimension n.

Definition 8 (IRNO type TP model) The convex polytopic TP model is an IRNO (Inverted and Relaxed Normal) type, if the smallest values of all weighting functions are 0, and the largest values of all weighting functions are the same for each dimension n.

4. TP MODEL BASED CONTROL DESIGN

A state feedback based control and observer design requiring to satisfy the convergence for stability $x(t) - \hat{x}(t) \to 0$ as $t \to \infty$ [12, 27, 28] are considered in the paper.

$$\begin{aligned}\begin{pmatrix}\dot{\hat{x}}\\ \hat{y}\end{pmatrix} &= S(\rho)\begin{pmatrix}\hat{x}\\ u\end{pmatrix} + \begin{pmatrix}K(\rho)\\ 0\end{pmatrix}(y - \hat{y})\\ u &= -F(\rho)\hat{x}\end{aligned} \tag{10}$$

The system $S(\rho)$, controller $F(\rho)$ and observer $K(\rho)$ take the following polytopic TP model structure:

$$S(\rho) = \mathcal{S} \underset{n\in N}{\boxtimes} w_n\left(\rho_n\right) \tag{11}$$

$$F(\rho) = \mathcal{F} \underset{n\in N}{\boxtimes} w_n\left(\rho_n\right) \tag{12}$$

$$K(\rho) = \mathcal{K} \underset{n\in N}{\boxtimes} w_n\left(\rho_n\right) \tag{13}$$

Such observer based state feedback control structure takes the parallel distributed compensation (PDC) schema [27, 28].

LMI Based Control Design

The state feedback controller vertex gains $F_{i_1,\,i_2,\,\ldots,\,i_N}$ stored in controller core tensor $\mathcal{F}$ are obtained based on the vertex systems $S_{i_1,\,i_2,\,\ldots,\,i_N}$ stored in system core tensor $\mathcal{S}$. The control design is done via the following LMI based design theorems guaranteeing asymptotic stability and a constraint on the control value:

Theorem 1: **Globally and asymptotically stable controller design**: Assume the polytopic model and a controller in a structure (10) is given. This state feedback control is globally and asymptotically stable if the matrices $P = P^T > 0$ and M_r exist, ($r = 1, \ldots, R$ where index r corresponds to that of Equation (2) and (3), and R denotes the number of LTI vertex systems) satisfying equations:

$$PA_r^T - M_r^T B_r^T + A_r P - B_r M_r < 0,$$

$$PA_r^T - M_s^T B_r^T + A_s P - B_r M_s + \\ PA_s^T - M_r^T B_s^T + A_s P - B_s M_r < 0$$

for $r < s \leq R$, except the pairs (r, s), such that $\forall \rho(t)$: $w_r(\rho(t))w_s(\rho(t)) = 0$, and where $M_r = F_r P$. The controller feedback gains can then be obtained from the solution of the above LMIs as $F_r = M_r P^{-1}$.

Theorem 2: **Constraint on the control value**: Assume, that $\|x(0)\| \leq \phi$, where $x(0)$ is unknown, but the upper bound ϕ is known. The constrain $\|u(t)\| \leq \mu$ is enforced at all times $t > 0$ if the LMIs

$$\phi^2 I \leq X$$

$$\begin{pmatrix} X & {M_r}^T \\ M_r & \mu^2 I \end{pmatrix} \geq 0$$

hold.

The observer vertex gains $K_{i_1, i_2, \ldots, i_N}$ stored in observer core tensor $\mathcal{K}$ are calculated in a similar fashion. The observer gains are obtained by applying the duality between the observer and controller design. Therefore, theorems 1-2 can be applied for the observer gain design.

Proofs of Theorems 1-2 can be found in [27, 28]. Furthermore, additional control objectives and constraints can be incorporated via LMI formulation or defining performance channels [27, 28].

5. TP Type qLPV Model of the mini MUTT Aircraft

A grid based LPV representation of the 33 state nonlinear ASE model of the mini MUTT aircraft can be derived by Jacobian linearization about a family of trim points as shown in [22]. In the present case the nonlinear model is trimmed and linearized for straight and level flight at various airspeeds at 281 equidistant grid points. The scheduling parameter is defined as $\rho = V_s \in [16 \ldots 30]\, m/s$. Note that since ρ depends on states u, v and w, the developed grid based LPV model of the mini MUTT aircraft belongs to the class of qLPV systems. The pole migration of the grid based qLPV model is given in Figure 2.

The grid based qLPV model serves as the starting point of TP model transformation. The TP model transformation is applied on the grid based qLPV model and the resulting highest 10 singular values after performing HOSVD are the following:

$$\begin{bmatrix} 43900.138 \\ 1347.518 \\ 33.851 \\ 0.896 \\ 0.029 \\ 0.002 \\ 2.439e-05 \\ 4.261e-06 \\ 1.575e-07 \\ 4.834e-09 \end{bmatrix}$$

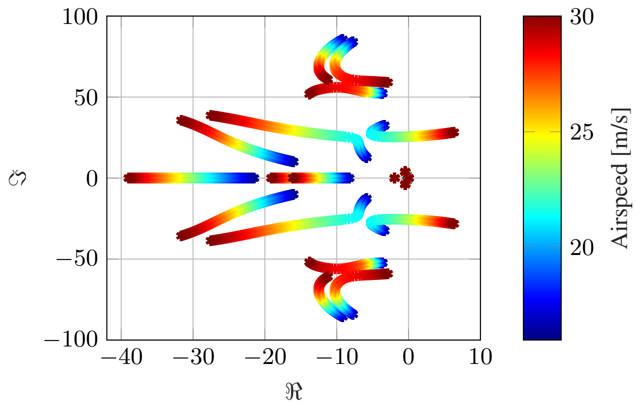

Figure 2: Pole migration of the mini MUTT aircraft

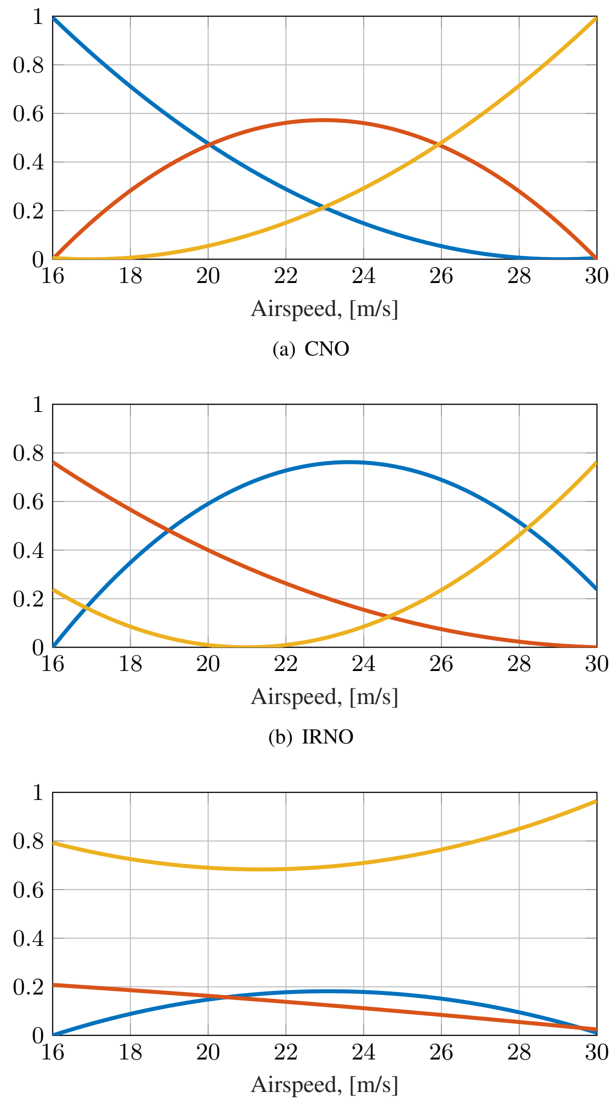

(a) CNO

(b) IRNO

(c) SNNN

Figure 3: Weighting functions

The magnitude of the singular values drop significantly after the third singular value. Therefore, keeping the first 3 singular values provides a polytopic model with 3 vertex systems.

Note, that this is only an approximate of the original qLPV system. CNO, IRNO and SNNN type polytopic models are derived. The vertexes are given with system matrices $S_{CNO}^{3\times51\times40}$, $S_{SNNN}^{3\times51\times40}$, and $S_{IRNO}^{3\times51\times40}$ and the weighting functions for the CNO, IRNO and SNNN type convex models are given in Figure 3.

It is important to point out that grid based LPV control synthesis is in general applied on a much coarser grid. On the other hand, executing TP model transformation over such dense grid can be executed in matter of a few seconds on a regular personal computer. Therefore, having a very fine grid density does not represent a high computational burden for TP model transformation.

Assessment of the TP type model—Since the TP model with 3 vertex systems is only an approximation of the grid based qLPV model, the accuracy of the TP model needs to be assessed. The accuracy of the TP type polytopic models is verified by reconstructing the 281 LTI systems at the original scheduling grid points. The reconstruction is done based on the 3 vertex systems and the CNO type weighting functions. The assessment is carried out by comparing a frequency based ν-gap metric ([29]) between the initial and the reconstructed LTI models. The ν-gap metric takes into account the feedback control objective. It takes values between zero and one, where zero is attained for two identical systems. A system P_1 that is within a distance ϵ to another system P_2 in the ν-gap metric, i. e. $\delta_\nu(P_1, P_2) < \epsilon$, will be stabilized by any feedback controller that stabilizes P_2 with a stability margin of at least ϵ. [29] A plant at a distance greater than ϵ from the P_2, on the other hand, will in general not be stabilized by the same controller. The ν-gap metric thus captures the likelihood that a feedback controller designed on the low order model will perform well on the full order model. The results of the ν-gap based accuracy of the approximate 3 vertex TP model can be seen in Figure 4.

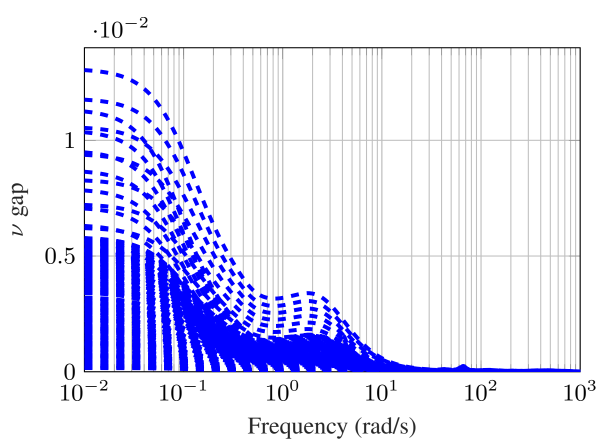

Figure 4: ν-gap metric of the TP models to the original qLPV model across the flight envelope

In addition, the Bode plots are also investigated. These show the input-output behavior from the aileron to the CG normal acceleration. Two grid points are investigated, one bellow and one above the flutter speed. The plots are given in Figure 5. It can be concluded that the TP model with 3 vertex systems describes the original grid based qLPV model with high accuracy. Therefore, it is not necessary to derive polytopic models of the mini MUTT aircraft based on more vertex systems.

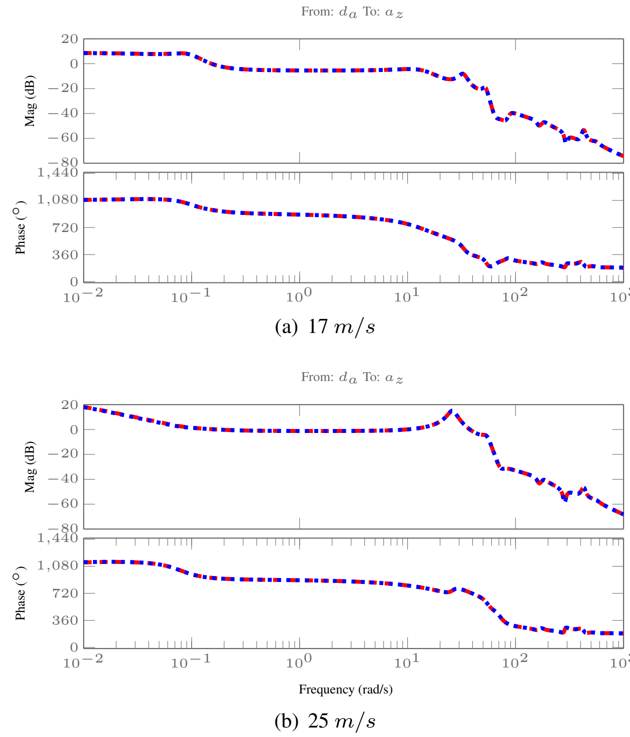

Figure 5: Bode diagrams: grid based qLPV model: (- - -), TP model: (⋯⋯)

Conservativeness analysis of the TP type qLPV systems—The TP type qLPV models are derived with the aim to have a set of models of the mini MUTT aircraft upon which polytopic type baseline, flutter suppression or integrated flight controllers can be derived. It is well known that the polytopic control design shows a certain degree of conservativeness. Polytopic control design results in a controller that guarantees stability and the prescribed control performance for all systems that are within the convex hull. The aim is to provide an insight into what systems are bounded by the CNO, IRNO and SNNN type convex hulls. This is done in the following way. In the first step, convex weights w_{conv} are defined. Since the weighting functions w_{CNO}, w_{IRNO} and w_{SNNN} are 3 dimensional, w_{conv} forms a plane as shown in Figure 6. The CNO and IRNO type weights of the mini MUTT aircraft are also given in the figure.

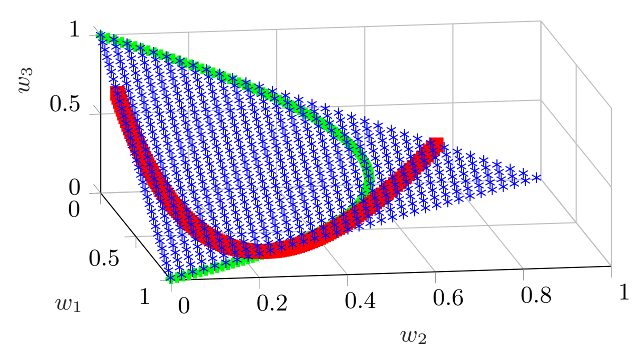

Figure 6: Weights for conservativeness analysis; 3 dimensional convex weights: (—∗—), CNO weights: (—+—), IRNO weights: (—⊡—)

In the second step, LTI systems are constructed from the

CNO, IRNO and SNNN type vertex systems with weights w_{conv}. Then the poles of these LTI systems are compared with the poles of the grid based qLPV systems. The pole migration of the flutter mode of the original grid based qLPV model and the convex combinations of the CNO and IRNO type convex hull is given in Figure 7. It can be concluded that the poles of the convex model cover a wider area than the grid based qLPV model. On the one hand, this leads to more conservative design. On the other hand, the resulting controller has some robustness properties against model uncertainties. In addition, the poles for the IRNO type convex hull cover a wider area compared to the CNO type convex hull. The SNNN type convex hull spreads out the poles even more, thus they are not given in the figure. In conclusion, it is expected that the IRNO and SNNN TP type qLPV models are too conservative for control design.

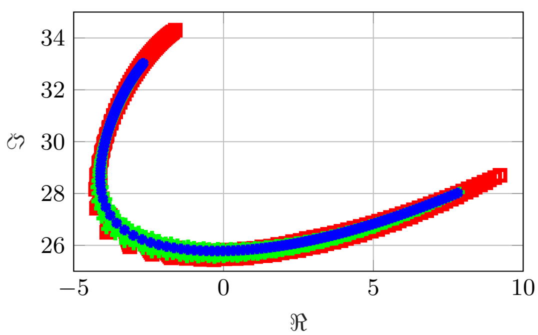

Figure 7: Pole migration of the flutter mode; grid based qLPV model: (—∗—), convex combinations for CNO type TP model: (—+—), convex combinations for IRNO type TP model: (—□—)

6. Numerical Results

Control Design with Different Weighting Functions

The LMI based state feedback control design is performed CNO, IRNO and SNNN type polytopic representation of the mini MUTT aircraft. The LMIs are defined based on Yalmip [30] and solved by the SDPT3 solver [31]. It needs to be emphasized that only the 4 flutter suppression control surfaces ($L1$, $L4$, $R1$ and $R4$) are utilized for the control design.

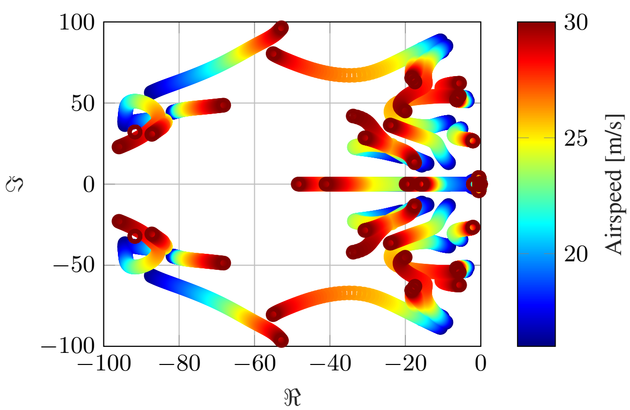

Figure 8: Pole migration of the closed loop

Determining the values for constraints ϕ and ν needs some consideration. The rigid body states of the mini MUTT aircraft have clear physical meanings. Therefore, it is straightforward to assume upper bound on their values. Determining upper bounds for the structural modes and the lag states is less intuitive. In this case, typical scenario open loop simulations are run to get a bound on $\|x\|$. As a result, $\phi = 8$ is chosen as an upper bound on $\|x\|$. An important aim of the control design is to keep the feedback gains F_i and the control signal u low. In case of the CNO type polytopic representation, the lowest bound on ν that leads to a feasible state feedback design was found to be $\nu = 0.2$. The SNNN and IRNO type representations did not lead to feasible control design. This is expected based in the considerations given in Section 5.

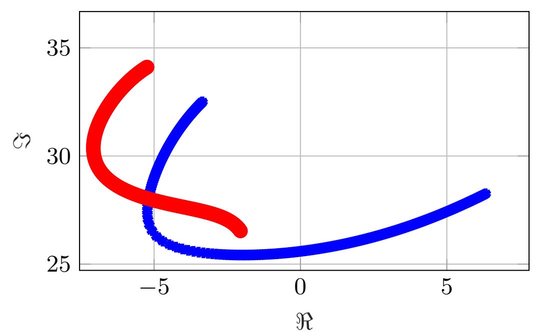

Figure 9: Open loop (—•—) and closed loop (—o—) flutter mode migration

The constraints for the observer design were chosen based on the same consideration as for the controller design. The bound on $\|x\|$ is kept constant at $\phi = 8$. A feasible observer gain is searched with the aim to keep constraint ν as low as possible. The observer design for the CNO and IRNO type representations resulted in feasible design with $\nu = 0.12$ while for the SNNN type representation with $\nu = 1.5$. The LMI based observer and controller designs run for approximately one minute on a typical personal computer.

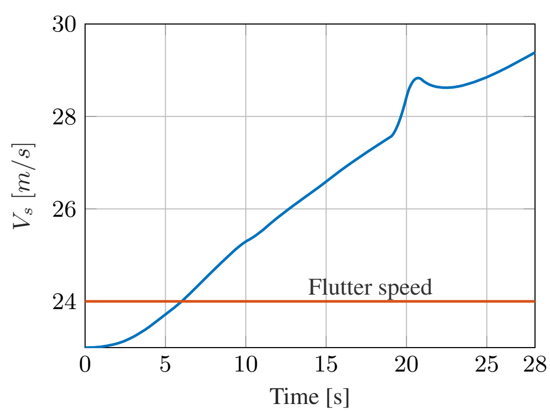

Figure 10: Airspeed V_s

The closed loop poles of the mini MUTT aircraft, evaluated at each grid point, are given in Figure 8. The observer and controller gains do not introduce very fast poles that can be challenging for implementation. Figure 9 shows how the flutter mode is shifted into the stable region. The resulting control design expands the flutter boundary from 24 m/s to 30 m/s. In addition, the spiral mode is also stabilized over the flight envelope.

Simulation Results

Time domain simulations are conducted to asses the effectiveness of the derived state feedback controller and observer structure. The qLPV state feedback controller and observer dynamics are connected with the 97 state full order nonlinear mini MUTT model. The simulation starts with straight and level flight trim condition at 23 m/s airspeed. The airspeed is then increased by adding a ramp signal to the throttle trim values so the airspeed of the aircraft goes beyond the flutter speed (Figure 10).

The control surfaces are kept at trim values scheduled by V_s. Wind gusts are simulated by applying $5°$ doublet disturbances on all control surfaces. The disturbances and the trim control surface values are shown in Figure 11.

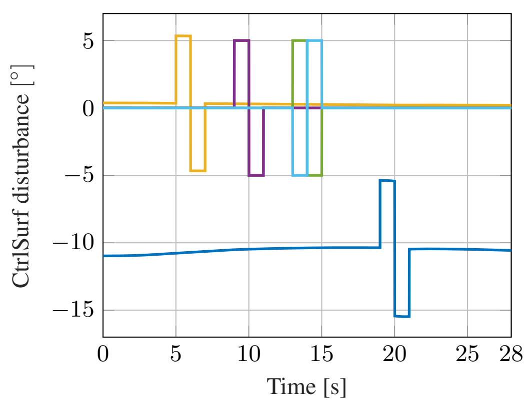

Figure 11: Disturbance acting on the control surface trim values: elevator (——), aileron (——), $L1$ (——), $R1$ (——), $L4$ (——) and $R4$ (——);

It is assumed that the flight controller has a time delay of 7.5 ms. This time delay is added to the control signal. In addition, it is assumed that the measured signals are noisy. The sensor noise characteristics are based on [32]. The simulations are carried out with the CNO type state feedback controller and CNO, IRNO and SNNN type observers. The CNO and IRNO type observers lead to very similar results, therefore only the CNO type observer results are shown. The SNNN type observer has higher gains which makes it more sensitive to sensor noise and results in unstable behavior.

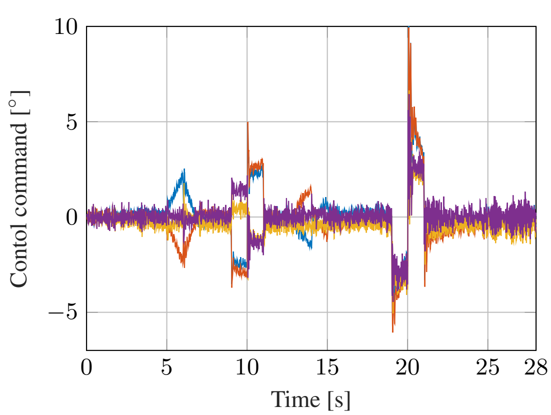

Figure 12: Control signal commands of the polytopic TP model controller with a CNO convex hull: $L1$ (——), $R1$ (——), $L4$ (——) and $R4$ (——);

The response of the mini MUTT aircraft to the excitations can be seen in Figure 13.

Evaluation of the Results and Future Steps

The simulation results show that the 33 state low order qLPV model based control structure is capable of stabilizing the 97 state high fidelity nonlinear model of the mini MUTT aircraft. Thus, the flutter boundary is expanded from 24 m/s to 30 m/s. The resulting control command values lie in a realistic interval of $\pm 8°$. In addition, the resulting control structure is not overly sensitive to computational time delays and sensor noise that inevitably appear in physical implementation cases. Some of the future steps of the research are the following:

- Include sensor dynamics and Padé approximation of the time delay in the qLPV model of the mini MUTT aircraft.
- Design dynamic LPV H_∞ flutter suppression controllers for both, grid based and polytopic LPV models of the mini MUTT aircraft.
- Investigate how the proposed flutter suppression controllers interact with the baseline controllers.
- Extend the proposed TP model based control design method for the FLEXOP aeroelastic aircraft [33].

7. CONCLUSIONS

The paper proposed TP model based polytopic modeling of ASE aircraft. The specific aircraft under consideration is the mini MUTT aircraft. The starting point of the polytopic modeling is a low order, 33 state grid based qLPV model. The polytopic model is obtained by TP model transformation. The number of vertex systems is determined by HOSVD-based singular values. TP model transformation resulted in a 3 vertex-based polytopic representation. The polytopic model is only an approximation of the grid based qLPV model. However, the ν-gap metric between the polytopic and grid based qLPV models is very low and the Bode plots are show almost identical input-output behavior for the grid based qLPV and the polytopic models. Several convex representations are derived based on which observer based stabilizing state feedback flutter suppression controllers are designed. The controller and observer take the same polytopic structure of the ASE model. It is shown that the various convex hulls influence the conservativeness of the resulting control design. The effectiveness of the resulting control structure is assessed by numerical simulations. The controller is connected with a high order, 97 state nonlinear ASE model. In addition, sensor noise and time delay is also included in the simulations. It is shown that the designed observer based controller successfully expands the flutter boundary from 24 m/s to 30 m/s.

ACKNOWLEDGMENTS

The research leading to these results is part of the FLEXOP project. This project has received funding from the European Unions Horizon 2020 research and innovation programme under grant agreement No 636307.

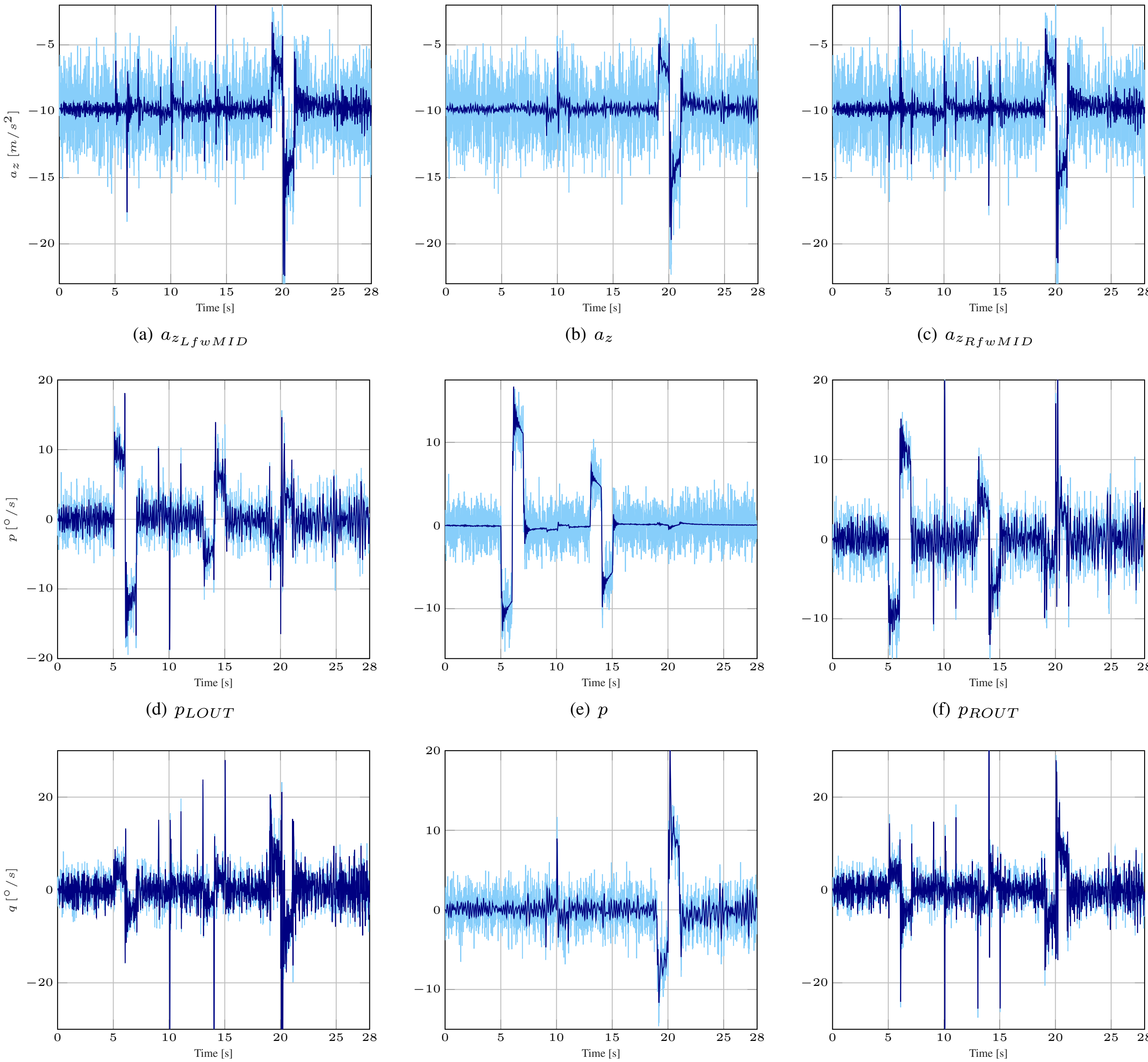

(a) $a_{z_{LfwMID}}$ (b) a_z (c) $a_{z_{RfwMID}}$

(d) p_{LOUT} (e) p (f) p_{ROUT}

(g) q_{LOUT} (h) q (i) q_{ROUT}

Figure 13: Response of the mini MUTT aircraft: signals with noise (——), signals without noise (——);

REFERENCES

[1] Y. Fung, *An introduction to the theory of aeroelasticity*, 1969.

[2] J. S. Shamma, "Analysis and design of gain scheduled control systems," Ph.D. dissertation, Massachusetts Institute of Technology, Cambridge, 1988.

[3] F. Wu, "Control of linear parameter varying systems," Ph.D. dissertation, Univ. California, Berkeley, 1995.

[4] A. Hjartarson, P. Seiler, and G. Balas, "LPV aeroservoelastic control using the LPVTools toolbox," in *AIAA Atmospheric Flight Mechanics Conference*, 2013, pp. Paper No. AIAA–2013–4742.

[5] ——, "Lpv robustness analysis of gain scheduled flight control for a aeroelastic aircraft," in *American Control Conference*, 2014, pp. 3778–3783.

[6] A. Packard, "Gain scheduling via linear fractional transformations," *Systems & Control Letters*, vol. 22, no. 2, pp. 79–92, Feb. 1994.

[7] J. Veenman and C. W. Scherer, "Stability analysis with integral quadratic constraints: A dissipativity based proof." IEEE, Dec. 2013, pp. 3770–3775.

[8] P. Apkarian, P. Gahinet, and G. Becker, "Self-scheduled h∞ control of linear parameter-varying systems: a design example," *Automatica*, vol. 31, no. 9, pp. 1251–1261, sep 1995.

[9] Yeung Yam and P. Baranyi, "Stabilizing controller by local linearization and SVD consolidation," vol. 2. IEEE, 2003, pp. 1482–1487.

[10] P. Baranyi, "TP model transformation as a way to LMI-based controller design," *IEEE Transactions on Industrial Electronics*, vol. 51, no. 2, pp. 387–400, 2004.

[11] L. De Lathauwer, B. De Moor, and J. Vandewalle, "A multilinear singular value decomposition," *SIAM Journal on Matrix Analysis and Applications*, vol. 21, no. 4, pp. 1253–1278, 2000.

[12] P. Baranyi, Y. Yam, and P. Varlaki, *Tensor product model transformation in polytopic model-based control*. Boca Raton, Fla.; London: CRC Press, 2006.

[13] P. Baranyi and B. Takarics, "Aeroelastic wing section control via relaxed tensor product model transformation framework," *Journal of Guidance, Control, and Dynamics*, vol. 37, no. 5, pp. 1671–1678, 2014.

[14] B. Takarics and P. Baranyi, "Tensor-product-model-based control of a three degrees-of-freedom aeroelastic model," *Journal of Guidance, Control, and Dynamics*, vol. 36, no. 5, pp. 1527–1533, 2013.

[15] S. Chumalee and J. F. Whidborne, "Gain-scheduled H_∞ control for tensor product type polytopic plants," *Asian Journal of Control*, vol. 17, no. 2, pp. 417–431, 2015.

[16] A. Szollosi and P. Baranyi, "Influence of the Tensor Product Model Representation of qLPV Models on the Feasibility of Linear Matrix Inequality based Stability Analysis," *Asian Journal of Control*, vol. n/a, no. n/a, pp. n/a–n/a, 2017.

[17] C. D. Regan and B. R. Taylor, "mAEWing1: Design, build, test - invited," in *AIAA Atmospheric Flight Mechanics Conference*. American Institute of Aeronautics and Astronautics, jan 2016.

[18] E. Burnett, C. Atkinson, J. Beranek, B. Sibbitt, B. Holm-Hansen, and L. Nicolai, "NDOF Simulation Model for Flight Control Development with Flight Test Correlation." American Institute of Aeronautics and Astronautics, Aug. 2010.

[19] J. J. Ryan and J. T. Bosworth, "Current and Future Research in Active Control of Lightweight, Flexible Structures Using the X-56 Aircraft." American Institute of Aeronautics and Astronautics, Jan. 2014.

[20] A. Kotikalpudi, "Robust flutter analysis for aeroservoelastic systems," Ph.D. dissertation, University of Minnesota, Twin Cities, 2017.

[21] A. Kotikalpudi, H. Pfifer, and G. Balas, "Unsteady aerodynamics analysis for a flexible unmanned aerial vehicle," in *AIAA Atmospheric Flight Mechanics Conference*, 2015.

[22] B. Takarics, B. Vanek, A. Kotikalpudi, and P. Seiler, "Flight control oriented bottom-up nonlinear modeling of aeroelastic vehicles," in *submitted to the IEEE Aerospace Conference*, 2017.

[23] P. Baranyi, *TP-Model Transformation-Based-Control Design Frameworks*. Cham, Switzerland: Springer International Publishing, 2016.

[24] P. Baranyi, L. Szeidl, P. Várlaki, and Y. Yam, "Definition of the HOSVD based canonical form of polytopic dynamic models," in *Proceedings of the 2006 IEEE International Conference on Mechatronics*, 2006, pp. 660–665.

[25] P. Baranyi, L. Szeidl, and P. Várlaki, "Numerical reconstruction of the HOSVD based canonical form of polytopic dynamic models," in *Proceedings of the 10th International Conference on Intelligent Engineering Systems*, 2006, pp. 196–201.

[26] L. Szeidl and P. Várlaki, "HOSVD based canonical form for polytopic models of dynamic systems," *Journal of Advanced Computational Intelligence and Intelligent Informatics*, vol. 13, no. 1, pp. 52–60, 2009.

[27] C. Scherer and S. Weiland, "Linear matrix inequalities in control," *Lecture Notes, Dutch Institute for Systems and Control, Delft, The Netherlands*, 2000, http://www.cs.ele.tue.nl/sweiland/lmi.htm.

[28] K. Tanaka and H. Wang, *Fuzzy control systems design and analysis: a linear matrix inequality approach*. John Wiley and Sons, Inc., U.S.A., 2001.

[29] G. Vinnicombe, "Measuring robustness of feedback systems," Ph.D. dissertation, Univ. Cambridge, Cambridge, 1993.

[30] J. LÖFBERG, "Yalmip: A toolbox for modeling and optimization in matlab," in *IEEE International Symposium on Computer Aided Control Systems Design*, 2004, pp. 284–289.

[31] K. Toh, R. Tütüncü, and M. Todd, "Sdpt 3 version 3. 02," *A Matlab software for semidefinite-quadratic-linear programming*, 2002.

[32] A. Dorobantu, W. Johnson, F. A. Lie, B. Taylor, A. Murch, Y. C. Paw, D. Gebre-Egziabher, and G. Balas, "An airborne experimental test platform: From theory to flight," in *2013 American Control Conference*. IEEE, jun 2013.

[33] FLEXOP, "Flutter Free FLight Envelope eXpansion for ecOnomical Performance improvement (FLEXOP)," Project of the European Union, Project ID: 636307, 2015-2018.

BIOGRAPHY

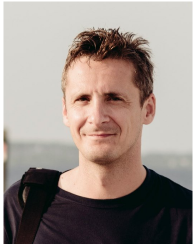

Béla Takarics *received his M.S. and Ph.D. degree in mechanical engineering from the Budapest University of Technology and Economics, Budapest, Hungary, in 2007 and 2012, respectively. He is currently a research fellow at the Systems and Control Lab (SCL) of the Research Institute for Computer Science and Control of the Hungarian Academy of Sciences (MTA SZTAKI). His research interests include linear parameter varying systems, IQC based robust control and aeroservoelastic systems.*

Alexandra Szöllősi *received her M.Sc. degree in electrical engineering from the Budapest University of Technology and Economics in 2015. She is a research fellow at the Systems and Control Lab (SCL) of the Research Institute for Computer Science and Control of the Hungarian Academy of Sciences (MTA SZTAKI) and a Ph.D. student at the Budapest University of Technology and Economics. Her research interests includes control theory of nonlinear systems, quasi- and Linear Parameter Varying systems (qLPV, LPV), Linear Matrix Inequality (LMI) based and Tensor Product model transformation based methods.*

Bálint Vanek *received his MSc degree in mechanical engineering from the Budapest University of Technology and Economics, Budapest, Hungary, in 2003 and a Ph.D. in aerospace engineering from the University of Minnesota, Department of Aerospace Engineering and Mechanics in 2008. He is currently a senior research fellow and leader of the Aerospace Guidance, Navigation, and Control Group at the Systems and Control Lab (SCL) of the Research Institute for Computer Science and Control of the Hungarian Academy of Sciences (MTA SZTAKI). His research interests include flight control, fault detection, unmanned aerial vehicles (UAVs), inertial and satellite navigation systems.*